

Conductivity and electronic conductivity of $\text{Li}_{0.3}(\text{MgCoNiCuZn})_{0.7}\text{O}$ - LiF high-entropy ceramics

YAZHOU KONG*, YOUFANG LIU

National & Local Joint Engineering Research Center for Mineral Salt Deep Utilization, Faculty of Chemical Engineering, Huaiyin Institute of Technology, Huaian 223003, P. R. China

$\text{Li}_{0.3}(\text{MgCoNiCuZn})_{0.7}\text{O}$ - $x\%$ LiF ($x=0, 5, 8, 10$) composite ceramics are synthesized by solid state reaction. Influence of sintering aids of LiF on the crystal structure, microstructure and conductivity for $\text{Li}_{0.3}(\text{MgCoNiCuZn})_{0.7}\text{O}$ is investigated. The ratio of electronic conductivity to total conductivity for $\text{Li}_{0.3}(\text{MgCoNiCuZn})_{0.7}\text{O}$ is 4.3%. Electronic conductivity in $\text{Li}_{0.3}(\text{MgCoNiCuZn})_{0.7}\text{O}$ cannot be ignored. The total conductivity of composite ceramics is improved with the addition of LiF sintering aids. The highest total electrical conductivity of $7.12 \times 10^{-5} \text{ S cm}^{-1}$ was obtained at $x=8$ at room temperature, with the activation energy of 0.31 eV. The electronic conductivity of $\text{Li}_{0.3}(\text{MgCoNiCuZn})_{0.7}\text{O}$ -8% LiF sample is $5.22 \times 10^{-7} \text{ S cm}^{-1}$, which is 100 times lower than its total electrical conductivity.

(Received March 18, 2022; accepted October 5, 2022)

Keywords: High-entropy ceramic, Composite, Rock salt, Solid electrolyte

1. Introduction

Fast lithium-ion conducting materials, also known as solid electrolyte, have attributed increasing interest due to the potential application in next-generation batteries, electrochemical sensors and electrochromic device [1]. Especially, the search for solid state electrolytes with high lithium-ion conductivity, good chemical/electrochemical stability is one of the important research interests for all-solid-state batteries [2, 3, 4]. A lot of oxides, sulfides and nitrides have been studied as solid state electrolytes for all-solid-state batteries, such as PEO-LiClO₄, LLTO ($\text{Li}_{0.33}\text{La}_{0.55}\text{TiO}_3$), LSTZ ($\text{Li}_{0.375}\text{Sr}_{0.4375}\text{Zr}_{0.25}\text{Ta}_{0.75}\text{O}_3$), LLZO ($\text{Li}_7\text{La}_3\text{Zr}_2\text{O}_{12}$), LATP ($\text{Li}_{1.3}\text{Al}_{0.3}\text{Ti}_{1.7}(\text{PO}_4)_3$), LGPS ($\text{Li}_{10}\text{GeP}_2\text{S}_{12}$), LIPON (Li-P-N-O) and LiOCl₃ [5, 6, 7, 8, 9, 10, 11]. However, LLTO, LSTZ and LATP are electrochemical unstable [12, 13, 14] in contact with metallic lithium, LGPS, LIPON and LiOCl₃ are hygroscopic and could react with water in air to produce impurities [15, 16, 17], Interfacial resistance of LLZO/electrodes is too large for application for solid state battery [18]. So far, no ideal solid electrolyte materials have been developed for lithium-ion battery.

Recently, researchers reported a new family of solid electrolyte with high entropy rock salt structure, $(\text{MgCoNiCuZn})_{1-x}\text{Li}_x\text{O}$ [19]. Lots of new properties such as super ionic conductivity and enhanced electrical conductivity have been discovered in high entropy rock salt ceramics [20, 21]. $(\text{MgCoNiCuZn})_{1-x}\text{Li}_x\text{O}$ ($x=0.33$) presents single rock salt structure and exhibits a high room

temperature conductivity of $1 \times 10^{-3} \text{ S cm}^{-1}$ with the activation energy of 0.20 eV. Conductivity of $(\text{MgCoNiCuZn})_{1-x}\text{Li}_x\text{O}$ ($x=0.33$) is 10 times higher than LiPON, LLZO and LSTZ [22, 23, 24]. While Li⁺ doped into $(\text{MgCoNiCuZn})\text{O}$ to form $(\text{MgCoNiCuZn})_{1-x}\text{Li}_x\text{O}$, oxygen vacancies were formed. Actually, oxygen vacancies are benefit to electronic conduction. Electronic conductivity is an important parameter for solid electrolyte. So, electronic conductivity of $(\text{MgCoNiCuZn})_{1-x}\text{Li}_x\text{O}$ should be studied.

LiF is an interesting and effective sintering aid for ceramic-type solid electrolyte. Xu [25] et al observed that LiF sintering aids increased the total ionic conductivity of $\text{Li}_{3/8}\text{Sr}_{7/16}\text{Hf}_{1/4}\text{Ta}_{3/4}\text{O}_3$ by about 1.5 times. Xiong [26, 27] et al reported significant enhancement of total ionic conductivity for LTP solid electrolyte with the addition of LiF sintering aids. LiF can improve the microstructure of solid electrolyte ceramics. In addition, LiF can decrease the sintering temperature of LATP ceramics.

In this study, high-entropy type $\text{Li}_{0.3}(\text{MgCoNiCuZn})_{0.7}\text{O}$ - $x\%$ LiF ($x=0, 5, 8, 10$) composites were prepared. LiF was added into $\text{Li}_{0.3}(\text{MgCoNiCuZn})_{0.7}\text{O}$ high entropy ceramic system as sintering aids. The influence of LiF sintering aids on the conductivity, electronic conductivity, microstructure and crystal structure for $\text{Li}_{0.3}(\text{MgCoNiCuZn})_{0.7}\text{O}$ was examined. Furthermore, electronic conductivity and its ratio in total conductivity for Li-doped $(\text{MgCoNiCuZn})\text{O}$ high-entropy ceramics was determined.

2. Experimental

High-entropy $\text{Li}_{0.3}(\text{MgCoNiCuZn})_{0.7}\text{O}$ - $x\%$ LiF ($x=0, 5, 8, 10$) ceramics were synthesized by the traditional solid state reaction method. NiO (AR, Aladdin reagent Ltd), Co_2O_3 (AR, Kelong reagent Ltd), MgO (AR, Yongda reagent Ltd), CuO (AR, Yongda reagent Ltd), LiF (AR, Aladdin reagent Ltd), ZnO (AR, Yongda reagent Ltd) and Li_2CO_3 (AR, Kelong reagent Ltd) were used as starting materials. All reagents were weighted in stoichiometric amounts and ball-milled for 24 h with ethanol as solvent on Mitr-YXQM-2 L planetary ball mill machine. The gained slurry was dried at 80°C for 24 h and then calcined at 900°C for 12 hours in air. The obtained powder was re-ball milled after adding different LiF contents for 8 h and then pressed into pellets with a diameter of 15 mm under 20 MPa. Finally, all the pressed pellets were sintered at 1000°C for 15 hours in air before air quenching.

The crystalline structure of sintered samples was detected by using X-ray diffraction (XRD) (Bruker D8 Advance diffractometer) in the 2θ range from 10° to 80° . Microstructure of the sintered pellets was observed using scanning electron microscopy (SEM, S-3000N). Silver pulp was used as blocking electrode for conductivity test. The conductivity of sintered pellets was measured via AC-impedance using CHI660E in the frequency range from 1 MHz to 1 Hz between 25°C and 120°C . The electronic conductivity of samples was measured by using DC polarization method (CHI660E electrochemistry workstation). The voltage was 4 V with a polarization time of 6000 s.

3. Results and discussion

Fig. 1 shows XRD profiles of $\text{Li}_{0.3}(\text{MgCoNiCuZn})_{0.7}\text{O}$ - $x\%$ LiF composites. $\text{Li}_{0.3}(\text{MgCoNiCuZn})_{0.7}\text{O}$ - $x\%$ LiF composite solid electrolytes show similar XRD patterns with pure $\text{Li}_{0.3}(\text{MgCoNiCuZn})_{0.7}\text{O}$. The main diffraction peaks for all samples corresponding to rock salt structure. Non peaks of LiF or other impurities were detected. The lattice parameters were measured and were listed in Table 1. The peak intensity of (111) was larger than (200) in $\text{Li}_{0.3}(\text{MgCoNiCuZn})_{0.7}\text{O}$ and $\text{Li}_{0.3}(\text{MgCoNiCuZn})_{0.7}\text{O}$ -5% LiF samples, but the effect was reversed in $\text{Li}_{0.3}(\text{MgCoNiCuZn})_{0.7}\text{O}$ -8% LiF and $\text{Li}_{0.3}(\text{MgCoNiCuZn})_{0.7}\text{O}$ -10% LiF. With the addition of low melting point LiF, the phase formation temperature of ceramics was decreased, which is benefit to the growth of (200) crystal face. LiF plays the role of sintering aids in the process of ceramic sintering.

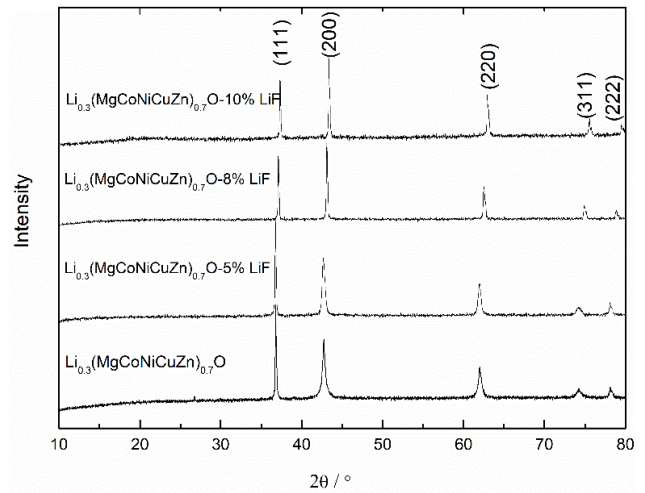


Fig. 1. XRD patterns of composite solid electrolyte

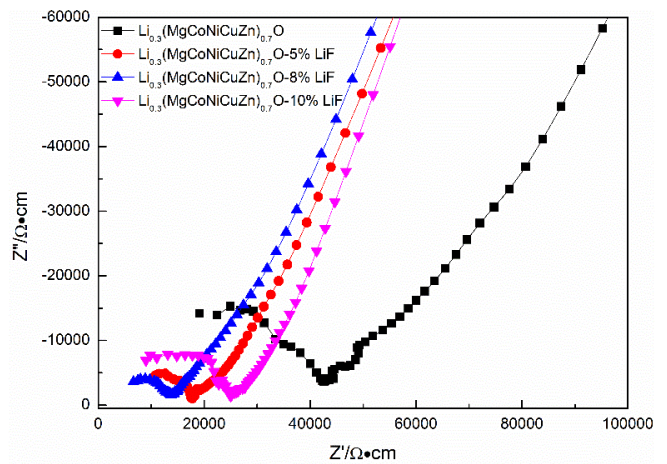


Fig. 2. Impedance profiles for $\text{Li}_{0.3}(\text{MgCoNiCuZn})_{0.7}\text{O}$ -LiF composites (color online)

Fig. 2 shows Nyquist plots of $\text{Li}_{0.3}(\text{MgCoNiCuZn})_{0.7}\text{O}$ - $x\%$ LiF composites sintered at 1000°C . These Impedance profiles have one semicircle only, which is attributed to the total resistance of corresponding solid electrolyte. The total conductivities were calculated by thickness (d), resistance (R) and surface area (S) of ceramic pellet as following:

$$\sigma = \frac{d}{R \times S} \quad (1)$$

The calculated results were listed in Table 1. The total conductivity (25°C) of $\text{Li}_{0.3}(\text{MgCoNiCuZn})_{0.7}\text{O}$ - $x\%$ LiF composites reach maximum of $7.12 \times 10^{-5} \text{ S cm}^{-1}$ at $x=8$. The total conductivity (25°C) of $\text{Li}_{0.3}(\text{MgCoNiCuZn})_{0.7}\text{O}$ -10% LiF was $3.83 \times 10^{-5} \text{ S cm}^{-1}$. The room temperature conductivity of $\text{Li}_{0.3}(\text{MgCoNiCuZn})_{0.7}\text{O}$ -8% LiF sample was higher than $\text{Li}_{0.3}(\text{MgCoNiCuZn})_{0.7}\text{O}$ -10% LiF sample.

Table 1. Lattice parameter, conductivity and activation energy of samples

Samples	Lattice parameters/Å	$\sigma_{total}/10^{-5} \text{ S cm}^{-1}$	$\sigma_{ele}/10^{-7} \text{ S cm}^{-1}$	$\frac{\sigma_{ele}}{\sigma_{total}}$	Activation energy/eV
$\text{Li}_{0.3}(\text{MgCoNiCuZn})_{0.7}\text{O}$	4.20301	2.22	9.45	4.3%	0.32
$\text{Li}_{0.3}(\text{MgCoNiCuZn})_{0.7}\text{O-5% LiF}$	4.20296	5.44	7.58	1.4%	0.34
$\text{Li}_{0.3}(\text{MgCoNiCuZn})_{0.7}\text{O-8% LiF}$	4.20294	7.12	5.22	0.8%	0.31
$\text{Li}_{0.3}(\text{MgCoNiCuZn})_{0.7}\text{O-10% LiF}$	4.20287	3.83	0.82	0.2%	0.29

The decrease of the total conductivity for $\text{Li}_{0.3}(\text{MgCoNiCuZn})_{0.7}\text{O-10% LiF}$ could be explained by the blocking effect for lithium ion conduction of excess LiF. A small amount of low melting point LiF could promote the sintering thus improve the total conductivity of composites. But LiF is insulant in nature, too much lithium fluoride is not conducive to the improvement of conductivity. So, the total conductivity of $\text{Li}_{0.3}(\text{MgCoNiCuZn})_{0.7}\text{O-10% LiF}$ is lower than $\text{Li}_{0.3}(\text{MgCoNiCuZn})_{0.7}\text{O-8% LiF}$.

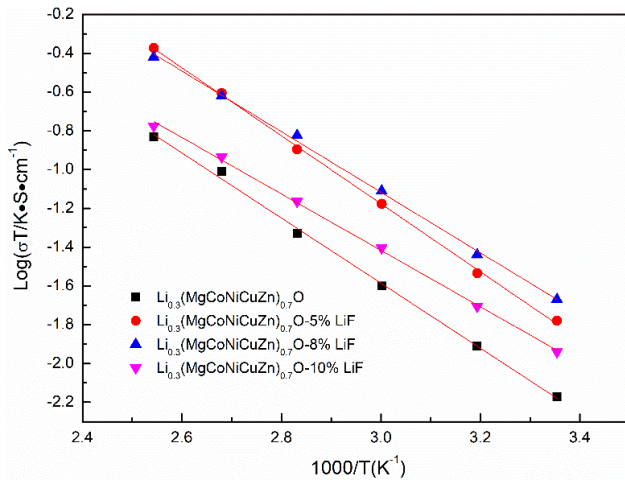


Fig. 3. Temperature dependence of conductivities of $\text{Li}_{0.3}(\text{MgCoNiCuZn})_{0.7}\text{O-}x\% \text{ LiF}$ composites (color online)

Fig. 3 shows the Arrhenius plots of $\text{Li}_{0.3}(\text{MgCoNiCuZn})_{0.7}\text{O-}x\% \text{ LiF}$ composites. The activation energies of $\text{Li}_{0.3}(\text{MgCoNiCuZn})_{0.7}\text{O-}x\% \text{ LiF}$ composites were calculated by:

$$\sigma T = \sigma_0 \exp\left(-\frac{Ea}{k_B T}\right) \quad (2)$$

The calculated results were listed in Table 1. Activation energies of pellets were obtained from the slope of Arrhenius plots ($\log \sigma T$ vs $1000/T$). As can be seen, the activation energies of all samples with different LiF amounts were around 0.3-0.4 eV, which is similar to

ceramic-type LLTO, LLZO and LATP solid electrolytes.

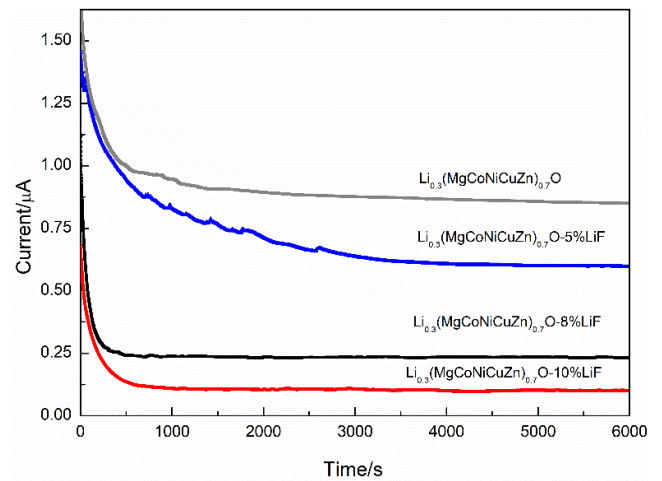


Fig. 4. Potentiostatic polarization curves of $\text{Li}_{0.3}(\text{MgCoNiCuZn})_{0.7}\text{O-}x\% \text{ LiF}$ using Li-ion blocking Ag electrodes (color online)

Fig. 4 shows the potentiostatic polarization current as a function of measuring time (current vs time) at 25 °C for $\text{Li}_{0.3}(\text{MgCoNiCuZn})_{0.7}\text{O-}x\% \text{ LiF}$. Due to the usage of Li-ion blocking Ag electrodes, the steady current shown in Fig. 4 was attributed to the electronic conduction in $\text{Li}_{0.3}(\text{MgCoNiCuZn})_{0.7}\text{O-}x\% \text{ LiF}$. The electronic conductivity (σ_{ele}) of samples was determined by:

$$\sigma_{ele} = \frac{I \times d}{U \times S} \quad (3)$$

The electronic conductivity of $\text{Li}_{0.3}(\text{MgCoNiCuZn})_{0.7}\text{O-}x\% \text{ LiF}$ was listed in Table 1. $\text{Li}_{0.3}(\text{MgCoNiCuZn})_{0.7}\text{O}$ presents an electronic conductivity of $9.45 \times 10^{-7} \text{ S cm}^{-1}$ at 25 °C. The ratio of electronic conductivity to total conductivity for $\text{Li}_{0.3}(\text{MgCoNiCuZn})_{0.7}\text{O}$ is 4.3%. Electronic conductivity in $\text{Li}_{0.3}(\text{MgCoNiCuZn})_{0.7}\text{O}$ cannot be ignored.

LiF has a low melting point of 848 °C and is a widely used as sintering aids for ceramic. Appropriate amount of LiF sintering aids is beneficial to the increment of total

conductivity of composite ceramics, but has little effect on electronic conductivity. However, LiF is insulating material in nature. The excess LiF could blocks ion and electron transport channels.

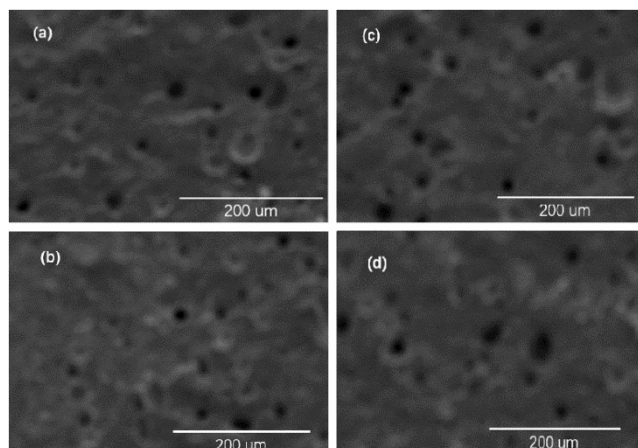


Fig. 5. SEM images of as-sintered composites

Fig. 5 shows SEM images of the cross-sectional morphology for $\text{Li}_{0.3}(\text{MgCoNiCuZn})_{0.7}\text{O}$ - $x\%$ LiF composites. A large number of holes were observed in all samples. This is attributed to the element loss during high temperature sintering, such as lithium. The porous structure is adverse to Li-ion conduction for ceramic-type solid electrolyte. The geometrical density of as-sintered samples was only about 70%, which is much lower than traditional ceramic electrolytes. A good ceramic-type solid electrolyte should have a density of more than 90%. To further improve the conductivity of $\text{Li}_x(\text{MgCoNiCuZn})_{1-x}\text{O}$ and related ceramics, the next step of the research could be focus on powder bed sintering, SPS sintering, hot pressing sintering and adding excess volatile elements.

4. Conclusions

Single phase Li-doped rock salt type high entropy ceramic $\text{Li}_{0.3}(\text{MgCoNiCuZn})_{0.7}\text{O}$ has been obtained successfully by solid state reaction with the addition of LiF as sintering aids. The highest total electrical conductivity of $7.12 \times 10^{-5} \text{ S cm}^{-1}$ was obtained at $x=8$ at room temperature, with the activation energy of 0.31 eV. The ratio of electronic conductivity to total electrical conductivity for $\text{Li}_{0.3}(\text{MgCoNiCuZn})_{0.7}\text{O}$ is 4.3%. $\text{Li}_{0.3}(\text{MgCoNiCuZn})_{0.7}\text{O}$ is not suitable as a solid electrolyte due to the high electronic conductivity. Appropriate amount of LiF sintering aids is beneficial to the increment of total conductivity of composite ceramics.

Acknowledgements

This work was supported by the Research Start-up Fund of Huaiyin Institute of Technology (Z301B20574), the fund of National & Local Joint Engineering Research Center for Mineral Salt Deep Utilization (SF201010).

References

- [1] J. Q. Zheng, Y. F. Li, R. Yang, G. Li, X. K. Ding, *Ceram. Int.* **43**, 1716 (2017).
- [2] J. C. Bachman, S. Muy, A. Grimaud, H. H. Chang, N. Pour, S. F. Lux, O. Paschos, F. Maglia, S. Lupart, P. Lamp, L. Giordano, Y. ShaoHorn, *Chem. Rev.* **116**, 140 (2016).
- [3] R. Chen, W. Qu, X. Guo, L. Li, F. Wu, *Materials Horizons* **3**, 487 (2016).
- [4] Z. Gao, H. Sun, L. Fu, F. Ye, Y. Zhang, W. Luo, Y. Huang, *Adv. Mater.* **30**, 705702 (2018).
- [5] K. Chen, M. Huang, Y. Shen, Y. Lin, C. W. Nan, *Electrochim. Acta* **80**, 133 (2012).
- [6] K. Kimura, K. Wagatsuma, T. Tojo, R. Inada, Y. Sakurai, *Ceram. Int.* **42**, 5546 (2016).
- [7] J. Xin, J. Lin, M. Yi, M. Chao, *Optoelectron. Adv. Mat.* **9**, 1458 (2015).
- [8] E. Zhao, F. Ma, Y. Jin, K. Kanamura, *J. Alloys Compd.* **680**, 646 (2016).
- [9] S. Hori, M. Kato, K. Suzuki, M. Hirayama, Y. Kato, R. Kanno, V. Sprenkle, *J. Am. Ceram. Soc.* **98**, 3352 (2015).
- [10] A. C. Kozen, A. J. Pearse, C. F. Lin, M. Noked, G. W. Rubloff, *Chem. Mater.* **27**(15), 5324 (2015).
- [11] X. Lu, G. Wu, J. W. Howard, A. Chen, Y. Zhao, L. L. Daemen, Q. Jia, *Chem. Commun. (Camb.)* **50**, 11520 (2014).
- [12] L. C. Zhang, J. F. Yang, Y. X. Gao, X. P. Wang, Q. F. Fang, C. H. Chen, *J. Power Sources* **355**, 69 (2017).
- [13] C. Chen, *Solid State Ionics* **167**, 263 (2004).
- [14] Y. Liu, C. Li, B. Li, H. Song, Z. Cheng, M. Chen, P. He, H. Zhou, *Adv. Energy Mater.* **8**, 1702347 (2018).
- [15] A. Manthiram, X. Yu, S. Wang, *Nat. Rev. Mater.* **2**, 16103 (2017).
- [16] C. Sun, J. Liu, Y. Gong, D. P. Wilkinson, J. Zhang, *Nano Energy* **33**, 363 (2017).
- [17] S. Li, J. Zhu, Y. Wang, J. W. Howard, X. Lü, Y. Li, R. S. Kumar, L. Wang, L. L. Daemen, Y. Zhao, *Solid State Ionics* **284**, 14 (2016).
- [18] M. He, Z. Cui, C. Chen, Y. Li, X. Guo, *J. Mater. Chem. A* **6**, 11463 (2018).
- [19] D. Bérardan, S. Franger, A. K. Meena, N. Dragoe, *J. Mater. Chem. A* **4**, 9536 (2016).
- [20] G. Yaohang, B. Ateer, W. Xuanyu, C. Yizhen, D. Liang, L. Xin, P. Haijun, L. Ying, Q. Xiwei, *Nanoscale* **14**, 515 (2022).
- [21] X. Huimin, X. Yan, D. Fu-zhi, W. Hongjie, S. Lei, M. Lei, Z. Guojun, W. Yiguang, Q. Xiwei, Y. Lei, W. Hailong, Z. Biao, L. Jianqiang, Z. Yanchun, *J. Adv.*

- Ceram. **10**, 385 (2021).
- [22] B. Put, P. M. Vereecken, J. Meersschaut, A. Sepulveda, A. Stesmans, ACS Appl. Mater. Interfaces **8**, 7060 (2016).
- [23] L. Zhang, X. Zhang, G. Tian, Q. Zhang, M. Knapp, H. Ehrenberg, G. Chen, Z. Shen, G. Yang, L. Gu, F. Du, Nat. Commun. **11**, 3490 (2020).
- [24] R. Inada, K. Kimura, K. Kusakabe, T. Tojo, Y. Sakurai, Solid State Ionics **261**, 95 (2014).
- [25] B. Xu, B. Huang, H. Liu, H. Duan, S. Zhong, C. A. Wang, Electrochim. Acta **234**, 1 (2017).
- [26] L. Xiong, Z. Ren, Y. Xu, S. Mao, P. Lei, M. Sun, Solid State Ionics **309**, 22 (2017).
- [27] K. Kwatek, W. Ślubowska, J. Trébosc, O. Lafon, J. L. Nowiński, J. Eur. Ceram. Soc. **40**, 85 (2020).

*Corresponding author: kongyazhou@hyit.edu.cn